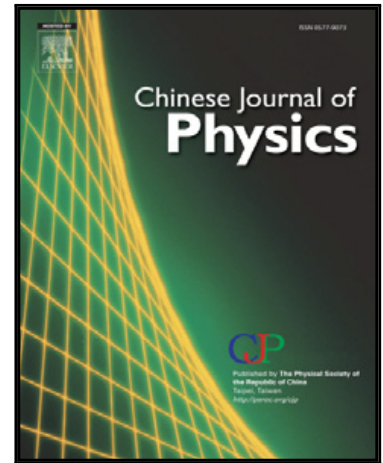


Journal Pre-proof

Polarization-dependent covalent organic framework saturable absorber and application of femtosecond fiber laser therein

Hsuan-Sen Wang , Ahmed F.M. EL-Mahdy , Shiao-Wei Kuo ,
Gong-Ru Lin , Chao-Kuei Lee

PII: S0577-9073(23)00221-6
DOI: <https://doi.org/10.1016/j.cjph.2023.10.040>
Reference: CJPH 2275



To appear in: *Chinese Journal of Physics*

Received date: 18 September 2023
Revised date: 22 October 2023
Accepted date: 28 October 2023

Please cite this article as: Hsuan-Sen Wang , Ahmed F.M. EL-Mahdy , Shiao-Wei Kuo , Gong-Ru Lin , Chao-Kuei Lee , Polarization-dependent covalent organic framework saturable absorber and application of femtosecond fiber laser therein, *Chinese Journal of Physics* (2023), doi: <https://doi.org/10.1016/j.cjph.2023.10.040>

This is a PDF file of an article that has undergone enhancements after acceptance, such as the addition of a cover page and metadata, and formatting for readability, but it is not yet the definitive version of record. This version will undergo additional copyediting, typesetting and review before it is published in its final form, but we are providing this version to give early visibility of the article. Please note that, during the production process, errors may be discovered which could affect the content, and all legal disclaimers that apply to the journal pertain.

© 2023 Published by Elsevier B.V. on behalf of The Physical Society of the Republic of China (Taiwan).

Highlights

- A covalent-organic framework (COF) saturable absorber (SA) is used in mode-locking.
- The nonlinear polarization rotation (NPR) dependence of the COF SA is studied.
- The mode-locking mechanism that relates saturable absorption and NPR is discussed.
- The results suggest the possible use of COFs as SAs in ultrafast photonics.

Polarization-dependent covalent organic framework saturable absorber and application of femtosecond fiber laser therein

Hsuan-Sen Wang, Ahmed F. M. EL-Mahdy, Shiao-Wei Kuo, Gong-Ru Lin^{}, and Chao-Kuei Lee^{*}*

Hsuan-Sen Wang, Chao-Kuei Lee

Department of Photonics

National Sun Yat-Sen University

Kaohsiung, 80424, Taiwan

E-mail: chuckcklee@yahoo.com

Shiao-Wei Kuo, Ahmed F. M. EL-Mahdy,

Department of Materials and Optoelectronic Science

National Sun Yat-Sen University

Kaohsiung, 80424, Taiwan

Gong-Ru Lin

Graduate Institute of Photonics and Optoelectronics and Department of Electrical

Engineering

National Taiwan University

Taipei 10617, Taiwan

E-mail: grlin@ntu.edu.tw

Abstract

Covalent organic frameworks (COFs) are materials that can be used in a wide variety of applications because of the nature of their ordered, crystalline, low-density, and porous structures. This work demonstrates the use of a π -electron-extended porphyrin/pyrene-linked COF (PorPh-PyTA-COF) as a saturable absorber (SA) in the

1.5 μm spectral region. The nonlinear optical absorption properties of this COF SA were studied and demonstrated a modulation depth of 0.8% and saturation intensity of 0.5 kW/cm^2 . Using the COF SA, the operation of a mode-locked erbium-doped fiber laser was realized with a pulse duration of 506 fs at 1570 nm. This is believed to be the first report of a COF-based mode-locked fiber laser operating in the near-infrared spectral range. Additionally, a 3.7 dB polarization-dependent loss was measured in the COF SA and its role in the mode-locking process was also discussed.

Keywords: Covalent organic framework; Porphyrin; mode-locked; Erbium-doped fiber laser

1. Introduction

Saturable absorbers (SAs) play an important role in enabling the operation of the mode-locked fiber laser [1]. SAs absorb low-intensity light but allow high-intensity light to pass. In general, these devices can be classified as either natural or artificial SAs. Artificial SAs, which include absorbers based on the nonlinear polarization rotation (NPR) technique and the nonlinear loop mirror, rely on the Kerr effect in optical fiber connections with other optical components to cause the SA action [2]. Typically, artificial SAs have required the formation of additional optical components, which has constrained their viability. Among the various material based SAs, semiconductor saturable absorber mirrors (SESAMs) are frequently used in laser pulsing [3]. However, SESAMs have several drawbacks that limit their application, including narrow operating bandwidths, high costs, slow recovery times, and complex setup requirements, and this has driven the exploration of new states for natural SAs. Previously, the use of inorganic materials, including graphene, transition metal disulfides (TMDs), topographic insulators (TIs), black phosphorus (BP), and MXenes, has been proposed, and these materials have been applied successfully in passively mode-locked fiber lasers for short pulse generation [4-9]. However, these materials still have certain limitations, such as optical nonlinearity engineering. In contrast, the molecular compositions and structures of organic materials are more diverse and can be adjusted flexibly to optimize their NLO properties. Among the approaches used for material optimization, it has been determined that the third-order NLO polarizability benefits from the extension of the π -electron delocalization in organic materials [10].

The porphyrin molecule, with its highly π -conjugated system, has previously been used widely in optoelectronic applications because of its extended π -electron

delocalization, which can be tuned by varying the nature of its substituents [11]. Nevertheless, tuning and enhancement of the material's NLO performance for use in practical device applications such as optical limiting, pulse compression, and SAs for ultrafast pulse generation by extending the π -electron delocalization in porphyrin remain desirable. An appropriate platform is required to enhance the material's NLO properties further. Covalent organic frameworks (COFs) provide an ideal platform for the design of ordered, crystalline, low-density, and porous materials that feature atomically exquisite integration of organic units that are built into extended two- and three-dimensional periodic structures. Because of their low density, large surface areas, chemical/thermal stabilities, and π -stacked architectures, COFs have drawn widespread attention in many research areas, including chemical sensors, electronics, catalysis, energy storage, luminescent devices, and nonlinear optics [12]. Therefore, porphyrin-linked COF has been proposed as a model system to enhance and tune the NLO response in porphyrins [13]. Despite the potential of these COFs, little research has been published about the saturable absorption of these materials and their application to laser pulsing. Furthermore, a mode-locked fiber laser based on a COF SA has yet to be realized.

In this work, we have developed a π -electron-extended porphyrin/pyrene-linked COF (PorPh-PyTA-COF) for use as a SA for ultrafast pulse generation in erbium-doped fiber lasers (EDFLs). Polyvinyl alcohol (PVA) is commonly used as a host polymer for SA devices due to its favorable mechanical properties and solvent compatibility [14]. To fabricate the COF-based SA, PorPh-PyTA-COF powder is embedded within a polyvinyl alcohol (PVA) film to fabricate a COF-based SA (COF-PVA SA). The saturable absorption properties and polarization dependence of the COF-PVA SA were then investigated. Additionally, the polarization-dependent loss within the COF-PVA SA, which can be attributed to its rotational stacking structure, has been characterized. A mode-locked EDFL based on a COF-PVA SA is demonstrated. The roles of saturable absorption and polarization-dependent loss are discussed. In addition to the fact that this is the first demonstration of a femtosecond fiber laser with a COF SA, this work provides a new window for the application of COFs in ultrafast photonics.

2. Fabrication and characterization of COF-based SAs

Since COFs were reported by Yaghi's group via the solvothermal method in 2005 [15], several approaches have been reported [16]. It's noteworthy that almost all COFs were synthesized under solvothermal conditions because of their simplicity [17]. As a result, the solvothermal method was employed to prepare the PorPh-PyTA-COF nanoparticles [18]. By using atomic force microscopy (AFM), the thickness of

these nanoparticles was determined to be approximately 180 nm, as depicted in Fig. 1(b). One should note that the PorPh-PyTA-COF nanoparticle used in this work has previously demonstrated a capability for Q-switched solid-state laser operation, indicating NLO functionality [18]. We embedded PorPh-PyTA-COF into a PVA film to fabricate the COF-PVA SA used in this work. The preparation process for the COF-PVA SA is illustrated in Fig. 1(a). First, the prepared PorPh-PyTA-COF powder was dispersed into deionized water, with sodium deoxycholate (SDC) acting as a surfactant. The PVA powder was then added to the COF dispersion, with subsequent magnetic stirring. Finally, the mixture was dropped onto a glass and dried at room temperature to form a solid SA film with a thickness of 100 μm . The linear transmittance of this film was assessed, as shown in Fig. 1(c). The results show that the COF effectively absorbs light over a broad frequency range. In contrast, the pure PVA film demonstrated high transmittance, indicating that it does not compromise the light-absorption properties of the COF-PVA SA. A piece of this film with dimensions of $\sim 1 \times 1 \text{ mm}^2$ was carefully cut out and then sandwiched between two fiber ferrules to act as the proposed SA.

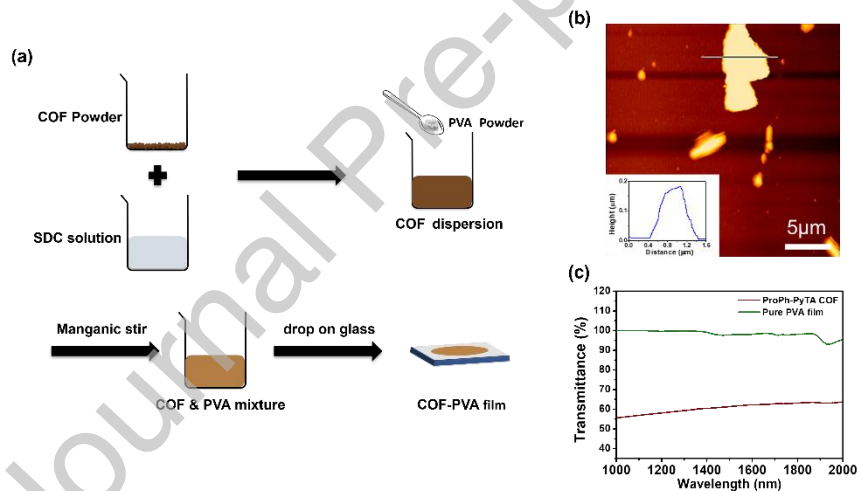


Figure 1. (a) Schematic diagram of the preparation of COF-PVA SA (b) AFM image of Porph-PyTA COF nanoparticle; inset: the height profile (c) Linear optical transmittance spectrum.

To investigate its NLO properties, the nonlinear optical absorption of the COF-PVA SA was measured using the power-dependent measurement system shown in Fig. 2(a). A homemade Q-switched laser operating at 1570 nm, with a pulse duration of 6.5 μs and a repetition rate of 15.9 kHz, was used as the laser pump source. Measurements were then performed by changing the input power using a variable optical attenuator. The input light was then divided into two parts via a connection with a 90:10 output coupler. The 90% component was intended for use in the characterization of the absorption, and the remaining 10% was used as a reference

signal. Using the simultaneously detected reference signal and the absorption results, the transmittance was estimated accordingly. Fig. 2(b). shows the experimental results and the corresponding fitting curve. The experimental results were fitted using the following formula [19]:

$$T(I) = 1 - \Delta T \cdot \exp\left(-\frac{I}{I_{\text{sat}}}\right) - T_{\text{ns}} \quad (1)$$

$T(I)$, ΔT , I_{sat} , I , and T_{ns} are the intensity-dependent transmittance, the modulation depth, the saturation intensity, the incident optical intensity, and the nonsaturable loss, respectively. The modulation of the COF-PVA-SA is approximately 0.8% with a saturation intensity of 0.5 kW/cm^2 . The COF-PVA SA showed ultralow saturation absorption for ultrafast laser generation, and this behavior has been observed previously [18]. In addition, the nonsaturable loss was 84.2% and can be attributed to coupling loss, which arises from the considerable thickness of the PVA film between the two fiber ferrules.

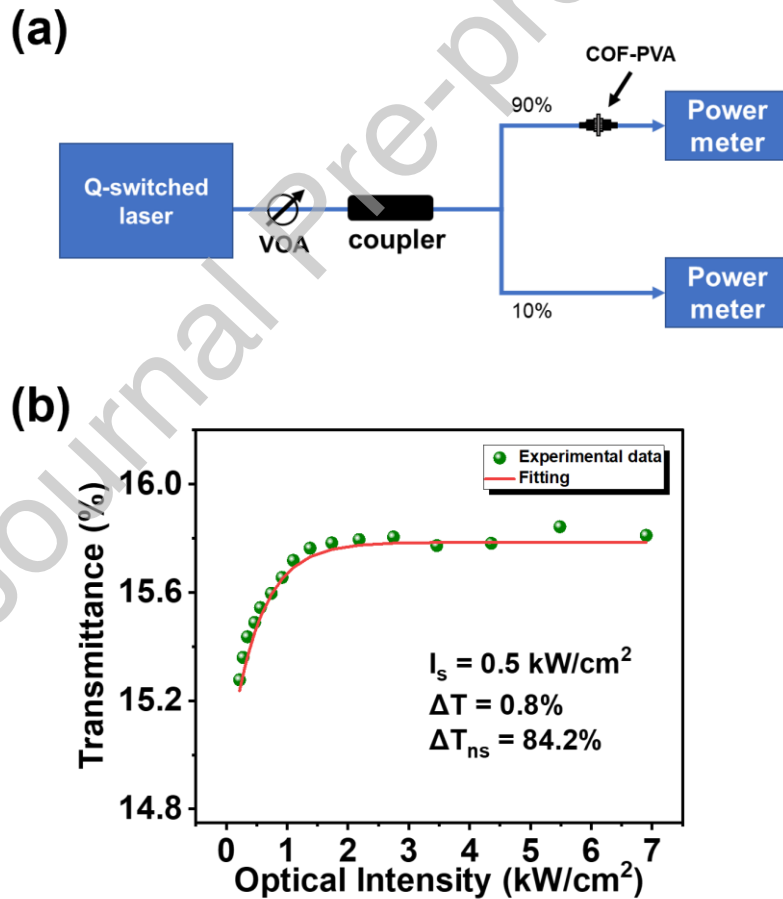


Figure 2. (a) Balanced twin-detector measurement system. (b) Experimental nonlinear optical absorption data and corresponding fitting curve.

3. Experiment Setup

After confirmation and characterization of the saturable absorption, a conventional ring fiber laser scheme was used to realize pulsed laser operation. The experimental setup for the EDFL based on the COF-PVA SA is shown in Fig. 3. The gain medium was a 2-m-long erbium-doped fiber (EDF) with a dispersion parameter of $-24.6 \text{ ps}^2/\text{km}$. A laser diode with a central wavelength of 976 nm was used as the pumping source. Wavelength division multiplexing (WDM) couplers were used to couple the pump laser beam into the EDF. A polarization-independent isolator (PI-ISO) was used to determine the intracavity propagation direction. A polarization controller (PC) controlled the intracavity polarization state. The total length of the single-mode fiber (SMF) used in the EDFL cavity was 8.1 m. A 1×2 optical coupler was used for 95% feedback and 5% output. The COF-PVA SA was inserted into the cavity after the PC. The total length of the single-mode fiber (SMF) with a dispersion parameter of $-23.6 \text{ ps}^2/\text{km}$ used in the EDFL cavity is 8.1 m. Combining the contribution from EDFA and SMF, the net cavity dispersion can be accordingly estimated to be around -0.24 ps^2 .

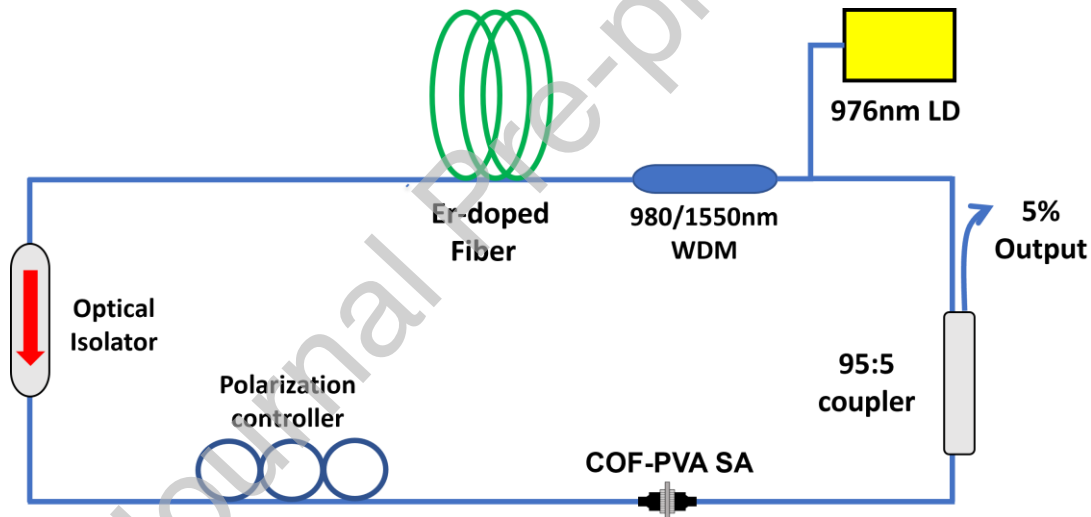


Figure 3. Schematic of erbium fiber laser setup with COF-PVA film.

4. Result and discussion

Despite the fact that both a metal-organic framework (MOF) SA-based mode-locked fiber laser and a COF-based Q-switched solid-state laser have been reported previously, there have been no reports to date about mode-locked operation using a COF SA.[20] Therefore, a pump power of 361 mW was applied, and self-starting mode-locking operation was realized in the EDFL with the COF SA by tuning the PC. Figure 4 summarizes the output properties of this mode-locking operation. The optical spectrum is given in Fig. 4(a). The central wavelength is 1570 nm, and the 3 dB bandwidth of the output is 5.2 nm. An unsymmetrical spectral sideband was observed. These sidebands are attributed to filtering effects induced by fiber birefringence [21].

An oscilloscope trace of the pulse train is shown in Fig. 4(b). The pulse interval is approximately 50 ns, which is consistent with the laser's cavity length of 10.1 m. The autocorrelator trace is shown in Fig 4(c). When the sech^2 pulse shape is used, the pulse duration is 506 fs. To provide further confirmation of the quality of the mode-locking operation, a radio-frequency (RF) spectrum analyzer was used to measure the RF spectrum of the mode-locked pulses. As shown in Fig. 4(d), the fundamental pulse repetition rate is 20 MHz. Additionally, the signal-to-noise ratio reaches 60 dB, indicating good mode-locking operation stability. The corresponding average output power, pulse energy, and peak power are 0.33 mW, 17 pJ, and 336 W, respectively. These characteristics confirm that the COF SA-based mode-locked fiber laser exhibits femtosecond-scale operation with high quality. To the best of our knowledge, this is the first time that COFs have been used as an SA for mode-locking of the fiber laser rather than for a conventional application, such as an optical limiter [22].

Typically, passive mode-locked fiber lasers can be realized using intracavity SAs or through a polarization modulation process [23]. Previously, the NPR mode-locking technique, which is sensitive to the polarization state in the cavity, has been investigated extensively, and it is used widely in fiber ring cavities [24]. The essential characteristic of this technique is that an intensity-dependent optical loss should be included within the cavity by inserting a polarization-dependent component into the cavity. The mode-locked state can then be achieved by tuning the PC at a specific pump power. To implement the NPR mode-locked laser, a polarizer is generally required. In 2010, Wu et al. demonstrated a mode-locked fiber laser based on the insertion of an optical component in the cavity with a 1.4 dB polarization-dependent loss (PDL) and achieved NPR mode locking without inserting a polarizer into the cavity [25]. Subsequently, Li et al. demonstrated an NPR mode-locked fiber laser by inserting a component with a 2 dB PDL into the cavity [26].

To gain a further understanding of the mode-locking mechanism in this work, the PDLs of the cavity components were first confirmed. After the COF-PVA SA was removed from the cavity, the laser's output power and its oscilloscope spectrum were observed for different polarization states by tuning the PC. Under the same pump power level, a maximum fluctuation of 0.2 dB in the output power was observed, thus indicating that the PDL of the cavity was less than 0.2 dB. Neither mode locking nor even Q-switching of a pulse was observed, despite the pump power being varied from zero to its maximum and the PC being tuned into different states simultaneously. This behavior can be attributed to the cavity being SA-free and the PDL being negligible.

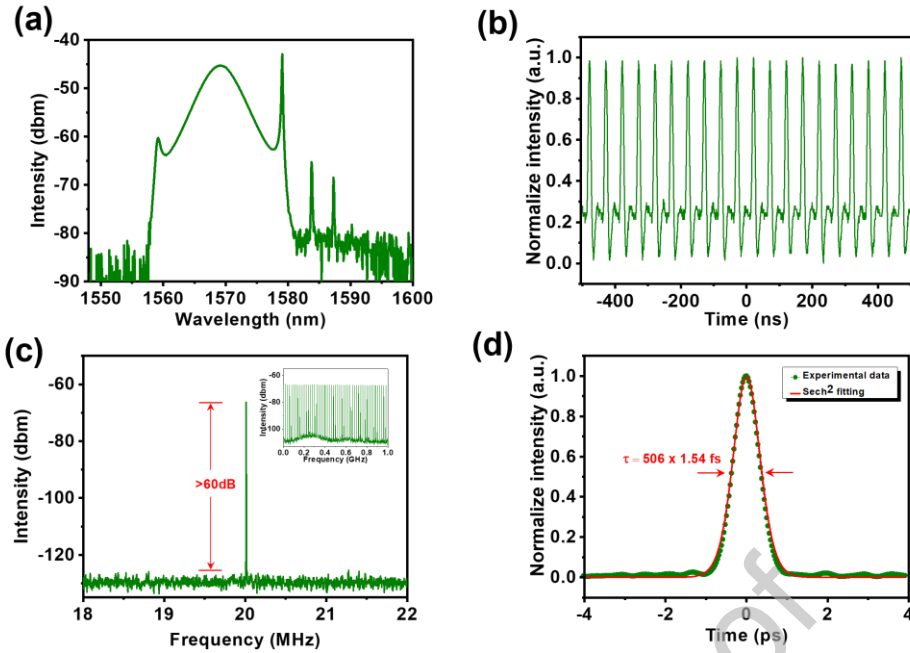


Figure 4. Properties of the mode-locked EDFL based on the COF-PVA SA. (a) Optical spectrum. (b) Pulse train. (c) Fundamental RF spectrum; inset: the broadband RF spectrum. (d) Autocorrelation traces.

Next, by removing the PC, we evaluated the performance of the laser with the COF-PVA SA. Self-starting Q-switched mode-locking operation was obtained when the pump power was increased to 206 mW. The typical Q-switching envelope versus pump power was also observed. Figure 5 summarizes the output properties of this Q-switched mode-locking operation. The center wavelength is 1569 nm, as shown in Fig. 5(a). An oscilloscope trace of the Q-switched mode-locking output pulses is shown in Fig. 5(b), which represents the incidence of the Q-switched mode-locking operation. As the pump power ranged from 240 to 361 mW, the repetition rate of the Q-switching envelope increased from 22.7 kHz to 32.4 kHz. In addition, the pulse duration decreased from 42.8 μ s to 26.4 μ s, as shown in Fig. 5(c). The laser output power and the pulse energy versus pump power characteristics are given in Fig. 5(d). The maximum output power and maximum pulse energy are 0.32 mW and 9.7 nJ, respectively, when pumped with a power of 361 mW. These results indicate that the COF SA alone cannot overcome the Q-switching instability without assistance from the PC at the maximum cavity energy. As a result, the PC is confirmed to play an essential role in the initiation mechanism of the CW mode-locking operation in this work. These results demonstrate that the mode-locking operation only exists for a cavity that includes the COF SA and the PC.

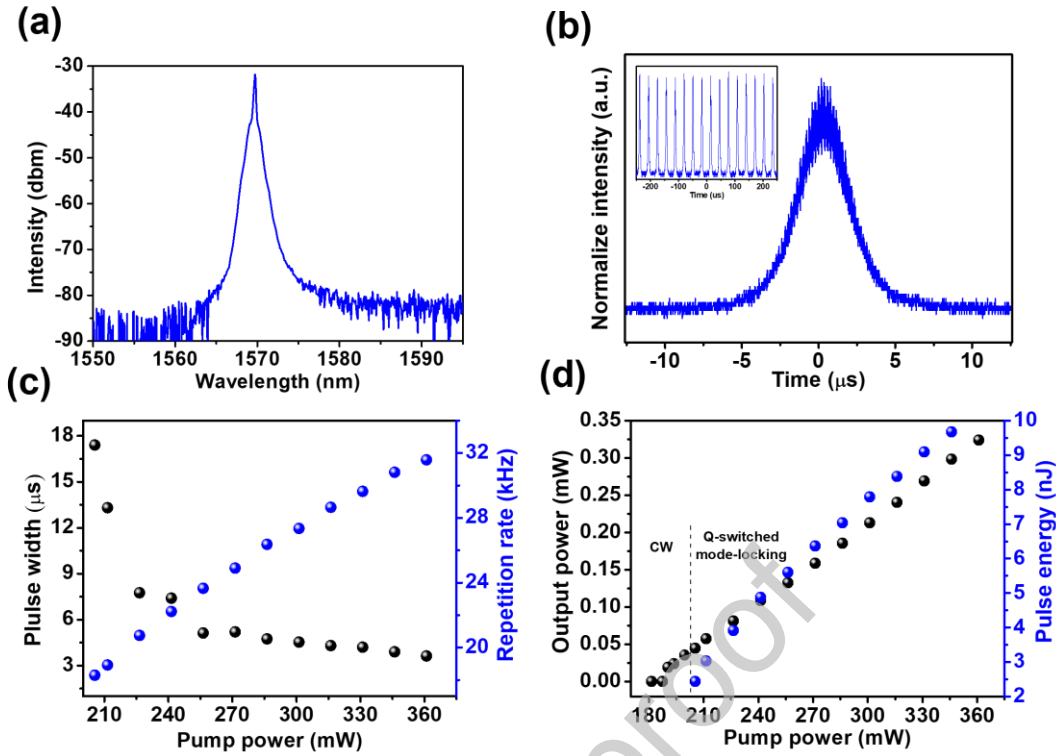


Figure 5. Properties of the Q-switched mode-locking EDFL based on the COF-PVA SA. (a) Optical spectrum. (b) Pulse trace, with an inset showing the pulse train. (c) Repetition rate and pulse duration, and (d) output power and single pulse energy versus pump power.

Previously, rotational stacking of a layered stable COF structure with optimized free energy has been reported, leading to the possibility of a PDL caused by the scattering difference between the left and right chirality [27]. To confirm and measure the polarization dependence of the COF-PVA SA, we therefore designed an optical system to characterize the PDL. A schematic diagram of this optical system is shown in Fig. 6(a). A 1570 nm continuous wave (CW) laser is used as the light source and is coupled to a fiber-to-fiber U-bench. The maximum measured optical power does not exceed 1 mW. A polarizer is inserted into the U-bench to control the polarization angle by rotating it. The other end of the U-bench connected a 90:10 output coupler (OC), and the COF-PVA SA was installed after the OC. As shown in Fig. 6(b), the COF-PVA film has a maximum transmittance of 27.4% and a minimum transmittance of 11.8% from a 0–360° linear polarization rotation. It is estimated using [Eq. (1)] that the PDL provided by the COF-PVA SA is 3.7 dB.

$$\text{PDL (dB)} = 10 \times \log\left(\frac{T_{\text{max}}}{T_{\text{min}}}\right) \quad (2)$$

To distinguish the originality of this PDL within the COF-PVA SA further, we also measured the polarization-dependent transmittance of a pure PVA film using the same measurement system. The transmittance of the pure PVA film is approximately

92% at any polarization angle, leading to the conclusion that the pure PVA film exhibits polarization independence. As a result, the PDL of the COF-PVA SA is contributed by the PorPh-PyTA-COF. By combining the requirements for mode-locking operation in this work with the nature of the PDL within the COF-PVA SA, we discern two key mechanisms in our laser pulsing operation: natural and artificial SA. Natural SA is typified by the inherent saturable absorption behavior demonstrated by the PorPh-PyTA-COF. In contrast, artificial SA is driven by the Kerr effect within the optical fiber. When this is paired with the inherent polarization dependence of the PorPh-PyTA-COF, it triggers additional saturable absorption behavior. Consequently, we posit that an EDFL, when equipped with the PorPh-PyTA-COF, uses a hybrid SA mechanism to enable the effective generation of the laser pulses. Previously, the hybrid mode-locked laser was proposed and demonstrated by several groups [28-30]. The results presented here show that the performance of this laser has been improved significantly compared with the mode-locked pulse obtained using natural or artificial SA alone. The natural saturable absorption and polarization dependence of PorPh-PyTA-COF provide a new way to generate hybrid mode-locked lasing without additional polarization-dependent optical components.

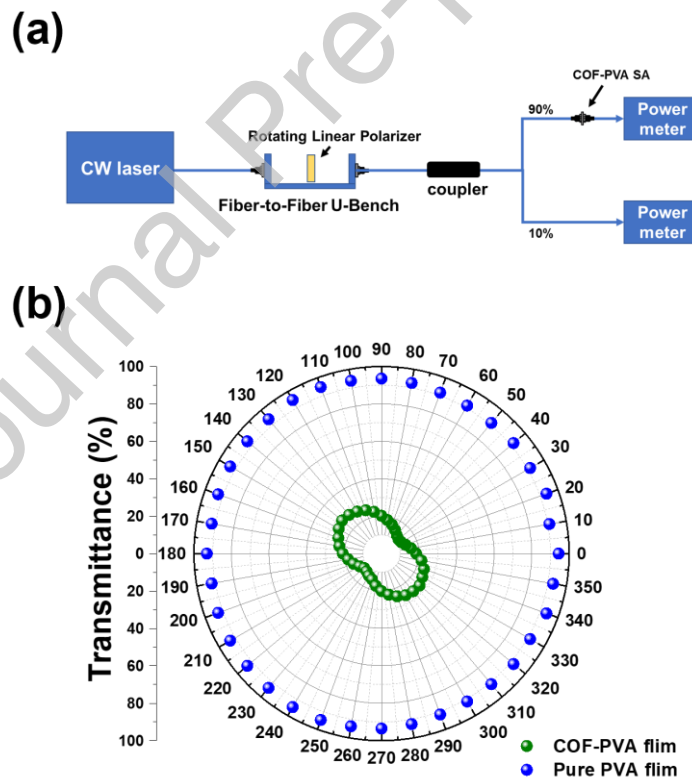


Figure 6. (a) Schematic of the optical system used to measure the polarization dependence of the COF-PVA SA. (b) Polarization dependence of the COF-PVA SA and the pure PVA film.

Although this is the first demonstration of a femtosecond fiber laser using the COF SA, the nonlinear optical properties and performance of mode-locked EDFLs based on organic-based SAs are shown in Table 1 to help visualize the impact of the results here. The mode-locking performance of the EDFL is similar to, if not better than, that demonstrated in previous reports of saturable absorbers based on other organic materials, indicating the promise of PorPh-PyTA-COF for applications in ultrafast photonics. Although the average output power is relatively low, it can be enhanced either by using an OC with a lower ratio or by fabricating thinner PVA film to reduce optical loss. Besides, it should be noted that the saturation intensity of PorPh-PyTA-COF is the lowest among the reported materials. The low saturation intensity observed can be ascribed to the substantial enhancement of optical nonlinearity facilitated by the extended π -electron delocalization framework [31]. This is beneficial for the generation of a high-repetition-rate mode-locked laser because the lower saturation intensity can reduce the characteristic pulse generation threshold.

Previously, PorPh-PyTA-COFs have shown exceptional thermal stability (up to 525 °C) and remarkable chemical stability in a variety of organic solvents as well as acidic and basic aqueous solutions. [18] Besides, Polyvinyl alcohol (PVA) is used as the host material in this work, serving to insulate the COF from environmental influences like water and oxygen. This ensures the long-term operational stability of the SA. To evaluate this, the time-dependent output spectrum was analyzed to illustrate the long-term stability of the mode-locking laser operation, see Fig. 7. Clearly, the mode-locking process remains almost unchanged over 6 hours. In addition to the stability, to further assess the optical damage threshold, a 1570 nm NPR mode-locked Er-doped fiber laser served as our light source. Even when subjected to the highest achievable peak intensity of 1.8 GW/cm², no optical damage was observed. This further confirms the laser's capability for long-term operation, which is crucial for real-world applications.

Various approaches have been proposed and demonstrated to generate mode-locked pulses in fiber lasers. NPR is a promising way to realize mode-locking operation within the fiber laser cavity. Typically, a polarization-dependent loss device, such as a polarizer, should be implanted inside the cavity [32]. However, additional cavity length or loss will be subsequently inevitable. Here, with the aid of the simultaneous existence of saturable absorption and polarization-dependent loss within the COF, the mode-locking operation was observed and characterized. This work provides a way for mode-locking the fiber laser without a conventional polarizer in the cavity and performs comparable laser pulse characteristics. In addition, this approach paves a way or direction to develop a new material system with chirality for

mode-locking fiber laser. Besides the various COF systems, the materials with chirality in nature will be a possible direction. The related work therefore starts and will have more convincing results soon.

Table 1. Comparison of all-fiber mode-locked performances using organic materials when operating in the 1.55 μm region

Material	Saturation intensity	Modulation (%)	Output power (mW)	Repetition rate (MHz)	Pulse energy (pJ)	Peak power (W)	Pulse duration (ps)	Ref.
PEDOT:PSS	0.14 MW/cm ²	22	6.89	2.44	2790	1603	1.74	33
Ni-MOF	19.8 GW/cm ²	5.2	0.54	6.47	83.5	111	0.75	34
DNA	281 MW/cm ²	0.4	4.2	29.29	143.4	341	0.42	35
DNA-CTMA	216 MW/cm ²	0.5	5.46	28.73	190	594	0.32	35
PorPh-PyTA-COF	0.5 kW/cm ²	0.8	0.33	20	16.5	33	0.51	This work

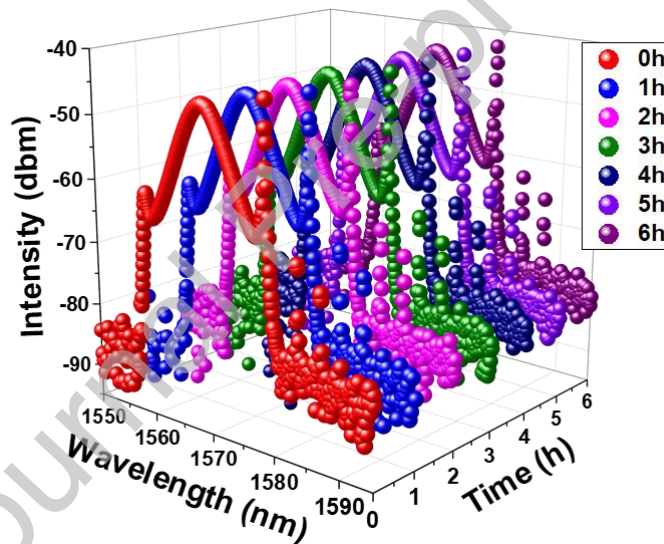


Figure 7. Long-term stability experiment results for the mode-locked EDFL based on COF-PVA SA over a 6 h period.

5. Conclusion

In this paper, a COF-based mode-locked EDFL has been demonstrated for the first time. We developed a mode-locked EDFL that operates at 1570 nm with a pulse duration of 506 fs. The nonlinear optical absorption of the PorPh-PyTA-COF SA is characterized by a 0.8% modulation depth with 0.5 kW/cm² saturation intensity. In addition to its saturable absorption properties, PorPh-PyTA-COF also shows polarization dependence, which induces additional saturable absorption behavior and

aids in the mode-locking operation. Our results show the enormous potential of PorPh-PyTA-COF with its unique optical properties for use in ultrafast pulse generation in fiber lasers and provide insights for further development of and research into the use of COFs in ultrafast optics.

Acknowledgment

This work is supported by the National Science and Technology Council, Taiwan (NSTC) under Contract No. NSTC109-2112-M-110-011-MY3.

Reference

- [1] Woodward, R., & Kelleher, E. (2015). 2D Saturable Absorbers for Fibre Lasers. *Applied Sciences*, 5(4), 1440–1456. <https://doi.org/10.3390/app5041440>
- [2] Haus, H. A., Ippen, E. P., & Tamura, K. (1994). Additive-pulse mode-locking in fiber lasers. *IEEE Journal of Quantum Electronics*, 30(1), 200–208. <https://doi.org/10.1109/3.272081>
- [3] Keller, U., Weingarten, K. J., Kartner, F. X., Kopf, D., Braun, B., Jung, I. D., Fluck, R., Honninger, C., Matuschek, N., & Aus der Au, J. (1996). Semiconductor saturable absorber mirrors (SESAMs) for femtosecond to nanosecond pulse generation in solid-state lasers. *IEEE Journal of Selected Topics in Quantum Electronics*, 2(3), 435–453. <https://doi.org/10.1109/2944.571743>
- [4] Bao, Q., Zhang, H., Wang, Y., Ni, Z., Yan, Y., Shen, Z. X., Loh, K. P., & Tang, D. Y. (2009). Atomic-Layer Graphene as a Saturable Absorber for Ultrafast Pulsed Lasers. *Advanced Functional Materials*, 19(19), 3077–3083. <https://doi.org/10.1002/adfm.200901007>
- [5] Chen, T.-H., Lin, C.-Y., Lin, Y.-H., Chi, Y.-C., Cheng, C.-H., Luo, Z., & Lin, G.-R. (2016). MoS₂ nano-flake doped polyvinyl alcohol enabling polarized soliton mode-locking of a fiber laser. *Journal of Materials Chemistry C*, 4(40), 9454–9459. <https://doi.org/10.1039/c6tc02623k>
- [6] Khazaeizhad, R., Kassani, S. H., Jeong, H., Yeom, D.-I., & Oh, K. (2014). Mode-locking of Er-doped fiber laser using a multilayer MoS₂ thin film as a saturable absorber in both anomalous and normal dispersion regimes. *Optics Express*, 22(19), 23732. <https://doi.org/10.1364/oe.22.023732>
- [7] Lin, Y.-H., Lin, S.-F., Chi, Y.-C., Wu, C.-L., Cheng, C.-H., Tseng, W.-H., He, J.-H., Wu, C.-I., Lee, C.-K., & Lin, G.-R. (2015). Using n- and p-Type Bi₂Te₃ Topological Insulator Nanoparticles to Enable Controlled Femtosecond Mode-Locking of Fiber Lasers. *ACS Photonics*, 2(4), 481–490. <https://doi.org/10.1021/acsphotonics.5b00031>
- [8] Zhang, M., Wu, Q., Zhang, F., Chen, L., Jin, X., Hu, Y., Zheng, Z., & Zhang, H. (2018). 2D Black Phosphorus Saturable Absorbers for Ultrafast Photonics. *Advanced Optical Materials*, 7(1), 1800224. <https://doi.org/10.1002/adom.201800224>
- [9] Jiang, X., Liu, S., Liang, W., Luo, S., He, Z., Ge, Y., Wang, H., Cao, R., Zhang, F., Wen, Q., Li, J., Bao, Q., Fan, D., & Zhang, H. (2017). Broadband Nonlinear Photonics in Few-Layer MXene Ti₃C₂Tx (T = F, O, or OH). *Laser & Photonics Reviews*, 12(2), 1700229.

<https://doi.org/10.1002/lpor.201700229>

- [10] NALWA, H. S. (2010). ChemInform Abstract: Organic Materials for Third-Order Nonlinear Optics. ChemInform, 24(35), no-no. <https://doi.org/10.1002/chin.199335316>
- [11] Senge, M. O., Fazekas, M., Notaras, E. G. A., Blau, W. J., Zawadzka, M., Locos, O. B., & Ni Mhuirheartaigh, E. M. (2007). Nonlinear Optical Properties of Porphyrins. Advanced Materials, 19(19), 2737–2774. <https://doi.org/10.1002/adma.200601850>
- [12] Chen, M., Li, H., Liu, C., Liu, J., Feng, Y., Wee, A. G. H., & Zhang, B. (2021). Porphyrin- and porphyrinoid-based covalent organic frameworks (COFs): From design, synthesis to applications. Coordination Chemistry Reviews, 435, 213778. <https://doi.org/10.1016/j.ccr.2021.213778>
- [13] Biswal, B. P., Valligatla, S., Wang, M., Banerjee, T., Saad, N. A., Mariserla, B. M. K., Chandrasekhar, N., Becker, D., Addicoat, M., Senkovska, I., Berger, R., Rao, D. N., Kaskel, S., & Feng, X. (2019). Nonlinear Optical Switching in Regioregular Porphyrin Covalent Organic Frameworks. Angewandte Chemie International Edition, 58(21), 6896–6900. <https://doi.org/10.1002/anie.201814412>
- [14] Sun, Z., Hasan, T., Torrisi, F., Popa, D., Privitera, G., Wang, F., Bonaccorso, F., Basko, D. M., & Ferrari, A. C. (2010). Graphene Mode-Locked Ultrafast Laser. ACS Nano, 4(2), 803–810. <https://doi.org/10.1021/nn901703e>
- [15] Côté, A. P., Benin, A. I., Ockwig, N. W., O’Keeffe, M., Matzger, A. J., & Yaghi, O. M. (2005). Porous, Crystalline, covalent organic frameworks. Science, 310(5751), 1166–1170. <https://doi.org/10.1126/science.1120411>
- [16] Abuzeid, H. R., EL-Mahdy, A. F. M., & Kuo, S.-W. (2021). Covalent organic frameworks: Design principles, synthetic strategies, and diverse applications. Giant, 6, 100054. <https://doi.org/10.1016/j.giant.2021.100054>
- [17] Deng, L., Zhang, J., & Gao, Y. (2019). Synthesis, Properties, and Their Potential Application of Covalent Organic Frameworks (COFs). IntechOpen. <https://10.5772/intechopen.82322>
- [18] Chen, K.-Y., Wang, H.-S., Su, S.-P., Kuo, S.-W., Lee, C.-K., & EL-Mahdy, A. F. M. (2022). Π Electron Extended Porphyrin Linked Covalent Organic Framework for a Q Switched All Solid State Laser. Advanced Photonics Research, 2200145. <https://doi.org/10.1002/adpr.202200145>
- [19] Chen, Y., Zhao, C., Huang, H., Chen, S., Tang, P., Wang, Z., Lu, S., Zhang, H., Wen, S., & Tang, D. (2013). Self-Assembled Topological Insulator: Bi_2Se_3 Membrane as a Passive Q-Switcher in an Erbium-Doped Fiber Laser. Journal of Lightwave Technology, 31(17), 2857–2863. <https://doi.org/10.1109/jlt.2013.2273493>
- [20] Jiang, X., Zhang, L., Liu, S., Zhang, Y., He, Z., Li, W., Zhang, F., Shi, Y., Lü, W., Li, Y., Wen, Q., Li, J., Feng, J., Ruan, S., Zeng, Y.-J., Zhu, X., Lu, Y., & Zhang, H. (2018). Ultrathin Metal-Organic Framework: An Emerging Broadband Nonlinear Optical Material for Ultrafast Photonics. Advanced Optical Materials, 6(16), 1800561. <https://doi.org/10.1002/adom.201800561>
- [21] Man, W. S., Tam, H. Y., Demokan, M. S., Wai, P. K. A., & Tang, D. Y. (2000). Mechanism of intrinsic wavelength tuning and sideband asymmetry in a passively mode-locked soliton fiber ring

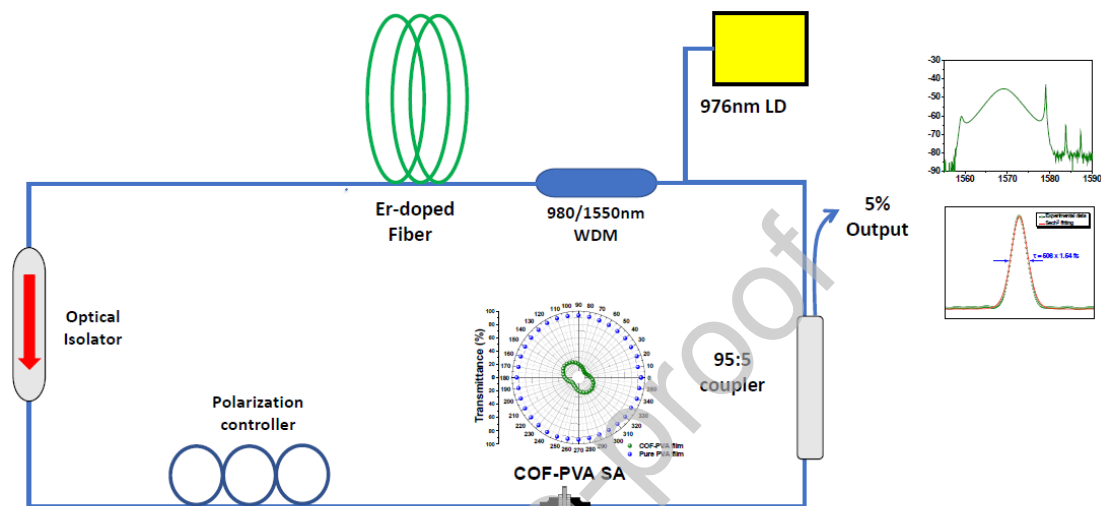
- laser. *Journal of the Optical Society of America B*, 17(1), 28. <https://doi.org/10.1364/josab.17.000028>
- [22] Liang, B., Zhao, J., Wang, J., Li, Y., Han, B., Li, J., Ding, X., Xie, Z., Wang, H., & Zhou, S. (2023). Nonlinear optical properties of porphyrin-based covalent organic frameworks determined by steric-orientation of conjugation. *Journal of Materials Chemistry C*, 11(9), 3354–3359. <https://doi.org/10.1039/d2tc05258j>
- [23] Sobon, G. (2016). Application of 2D Materials to Ultrashort Laser Pulse Generation. InTech. <https://doi.org/10.5772/63336>
- [24] Li, G., Yan, X., Kong, J., & Zhao, L. (2020). Passive mode locking in fiber lasers due to the polarization-dependent losses. *Applied Optics*, 59(33), 10201. <https://doi.org/10.1364/ao.411932>
- [25] Wu, X., Tang, D. Y., Zhao, L. M., & Zhang, H. (2010). Mode-locking of fiber lasers induced by residual polarization dependent loss of cavity components. *Laser Physics*, 20(10), 1913–1917. <https://doi.org/10.1134/s1054660x10190187>
- [26] Li, G., Chen, Y., Yan, X., & Zhao, L. (2018). Passive mode locking resulting from weak polarization dependence based on evanescent field interaction with a monolayer graphene absorber. *Applied Optics*, 57(13), 3507. <https://doi.org/10.1364/ao.57.003507>
- [27] Mohamed, M. G., Lee, C.-C., EL-Mahdy, A. F. M., Lüder, J., Yu, M.-H., Li, Z., Zhu, Z., Chueh, C.-C., & Kuo, S.-W. (2020). Exploitation of two-dimensional conjugated covalent organic frameworks based on tetraphenylethylene with bicarbazole and pyrene units and applications in perovskite solar cells. *Journal of Materials Chemistry A*, 8(22), 11448–11459. <https://doi.org/10.1039/d0ta02956d>
- [28] Jin, L., Zhang, Q., Zhang, B., Gao, Z., Yang, S., & Li, L. (2023). Numerical analysis of hybrid mode-locking stability in a Ho-doped fiber laser. *Optics Express*, 31(2), 1141. <https://doi.org/10.1364/oe.478860>
- [29] Pang, L., Wang, R., Li, L., Wu, R., & Lv, Y. (2020). Hybrid mode-locked fiber laser with Fe₃O₄ nanoparticles. *Infrared Physics & Technology*, 110, 103444. <https://doi.org/10.1016/j.infrared.2020.103444>
- [30] Lyu, Y., Li, J., Hu, Y., Wang, Y., Wei, C., & Liu, Y. (2017). Theoretical Comparison of NPR and Hybrid Mode-Locked Soliton Thulium-Doped Fiber Lasers. *IEEE Photonics Journal*, 9(1), 1–11. <https://doi.org/10.1109/jphot.2017.2653860>
- [31] Nalwa, H.S. (1993). Organic Materials for Third-Order Nonlinear Optics, *Advanced Materials*, 5(5), pp. 341–358. <https://doi.org/10.1002/adma.19930050504>
- [32] Haus, H. A., Ippen, E. P., & Tamura, K. (1994). Additive-pulse modelocking in fiber lasers. *IEEE Journal of Quantum Electronics*, 30(1), 200–208. <https://doi.org/10.1109/3.272081>
- [33] Al-Hiti, A. S., Tiu, Z. C., Yasin, M., & Harun, S. W. (2022). Ultrafast fiber laser at 1570 nm based on organic material as saturable absorber. *Scientific Reports*, 12(1), 13288. <https://doi.org/10.1038/s41598-022-17724-9>
- [34] Jiang, X., Zhang, L., Liu, S., Zhang, Y., He, Z., Li, W., Zhang, F., Shi, Y., Lü, W., Li, Y., Wen, Q., Li, J., Feng, J., Ruan, S., Zeng, Y.-J., Zhu, X., Lu, Y., & Zhang, H. (2018). Ultrathin Metal-Organic Framework: An Emerging Broadband Nonlinear Optical Material for Ultrafast Photonics. *Advanced*

Optical Materials, 6(16), 1800561. <https://doi.org/10.1002/adom.201800561>

[35] Al-Hiti, A. S., Yasin, M., Tiu, Z. C., & Harun, S. W. (2022). Soliton picosecond pulse generation with a spin-coated PEDOT: PSS thin film. *Journal of Luminescence*, 247, 118879.

<https://doi.org/10.1016/j.jlumin.2022.118879>

Graphical Abstract



Declaration of interests

The authors declare that they have no known competing financial interests or personal relationships that could have appeared to influence the work reported in this paper.

The authors declare the following financial interests/personal relationships which may be considered as potential competing interests: